

Synthesis, structure, electrochemistry and ROMP-activity of new ferrocenyl analog of Grubbs' metathesis catalyst

Tarun K. Maishal ^a, Biplab Mondal ^b, Vedavati G. Puranik ^c, Prakash P. Wadgaonkar ^d,
Goutam Kumar Lahiri ^b, Amitabha Sarkar ^{a,*}

^a Divisions of Organic Chemistry (Synthesis), National Chemical Laboratory, Pune 411008, India

^b Department of Chemistry, Indian Institute of Technology, Bombay, Powai, Mumbai 400 076, India

^c Physical Chemistry, National Chemical Laboratory, Pune 411008, India

^d Polymer Chemistry Division, National Chemical Laboratory, Pune 411008, India

Abstract

Treatment of [(PCy₃)₂Cl₂Ru=CH-Ph] (**I**) with vinylferrocene **1** and 1-ferrocenyl-1,3-butadiene **2** yielded solid products. These new complexes were characterized by ¹H NMR, ³¹P NMR and ¹³C NMR spectroscopy. X-ray crystal structures of both the complexes have been solved. The crystal structure of **II** confirmed the assigned structure and revealed existence of two sets of intermolecular C-H-Cl(M) type interactions, viz. (Ru)Cl-H-C(ferrocene) and (Ru)Cl-H-CHCl₂. The air-stable, dark solid **II** is an efficient catalyst for ring-opening metathesis polymerization (ROMP) of cyclopentene, norbornene and cycloocta-1,5-diene. Electrochemical behavior of the complexes clearly reflects electronic communication between two metal centers.

Keywords: Metathesis; Ruthenium Carbene; Ferrocene; Non-covalent interaction; Electrochemistry; Ring-opening metathesis polymerization

1. Introduction

Heteronuclear, mixed-valence organometallic compounds [1] are often synthesized in order to gain insight into the electronic structure of mixed-valent compounds, the factors affecting electron transfer between interacting sites, and the extent of delocalization of the valence electrons [2]. Redox properties of such compounds often differ from the properties of component redox sites. Mixed-valence compounds are of considerable interest in the context of superconducting or semiconducting materials and biologically relevant mixed-valence compounds [3]. Besides, these compounds may have possible

applications in electrocatalysis and solar energy [4]. Non-linear optics is another area where such polarizable molecules have been exploited [5].

The ferrocene (Fc) moiety, a versatile, redox-active electro-donor component, is an attractive candidate for incorporation into bimetallic or polymetallic scaffolds [6]. The conjugated ferrocene derivatives are being tested for second- and third-order optical non-linearity for potential application in optical data storage and processing [7].

This paper illustrates a very simple strategy to build up bimetallic complexes from monometallic counterparts in a single step using alkene-metathesis as the key stoichiometric reaction [8]. Redox properties of these complexes corroborate existence of internuclear electronic communication. In addition, both complexes described herein are potential catalysts for ring-closing metathesis (RCM), cross-metathesis (CM), ring-opening

cross-metathesis (ROCM) [8c] and ring-opening metathesis polymerization (ROMP).

2. Results and discussion

2.1. Synthesis and characterization of Ru–Fc complexes

Metathesis of a metal-alkylidene moiety with an alkene that is linked to an organic π -donor ligand attached to another metal, was used as a general strategy to prepare bimetallic complexes. For the complexes described herein, the alkene group is conjugated to the π -donor ligand of the second metal.

The starting material was Grubbs' metathesis catalyst **I**, which was prepared following the procedure described in the literature [9]. Replacement of the benzylidene group of the complex by a different terminal alkene was also reported in the same paper. This strategy was clearly successful in our hands for the preparation of two new complexes. The reaction between vinylferrocene **1** and 1-ferrocenyl-1,3-butadiene [10] **2** (derived from ferrocenecarboxaldehyde) and $(\text{PCy}_3)_2\text{Cl}_2\text{Ru}=\text{C}(\text{H})\text{Ph}$ (**I**) afforded complexes with structure $(\text{PCy}_3)_2\text{Cl}_2\text{Ru}=\text{C}(\text{H})\text{Fc}$ (**II**) and $(\text{PCy}_3)_2\text{Cl}_2\text{Ru}=\text{C}(\text{H})\text{C}(\text{H})=\text{C}(\text{H})\text{Fc}$ (**III**) respectively (Scheme 1). In a typical procedure, the alkene was added to a dichloromethane solution of complex **I** at ambient temperature. After the starting complex was completely consumed (TLC, ≈ 30 – 40 min), dichloromethane was evaporated in vacuo. Addition of methanol to the residue afforded red to dark brown powders in 87–92% isolated yield. No $\text{Ru}=\text{CH}_2$ product was detected, indicating that the reactions were highly regioselective.

The ^1H , ^{13}C and ^{31}P NMR spectra for complexes **II** and **III** strongly suggested that their structures are very similar to their precursor **I**. In both instances, singlet ^{31}P signals (34.40 and 35.13 ppm) indicate that phosphine ligands are oriented *trans* to each other and the alkylidene moiety bisects the P–Ru–P plane [9]. The alkylidene methine signals for complexes **II** and **III** (19.0 and 18.5 ppm) are shielded with respect to corresponding proton

resonance in complex **I** (20.02 ppm). Similarly, ^{13}C chemical shifts for the carbene carbon in these new complexes (288 and 292 ppm) are shielded relative to the corresponding signal of carbene **I** (295 ppm). The structural similarities were later confirmed by X-ray crystallography.

2.2. Crystal structure

Initially, the complexes were isolated as microcrystalline solids that were not suitable for X-ray structure determination. After several unsuccessful attempts, X-ray grade crystals were obtained by slow diffusion of methanol into a concentrated solution of complex **II** in dichloromethane at low temperature (-78 °C). Similarly, slow evaporation of dichloromethane under reduced pressure from methanol–dichloromethane solution of **III** at 0 °C afforded the deep reddish-brown crystal of **III**. ORTEP diagrams of the complex **II** and **III** are shown in Figs. 1 and 2, and data collection

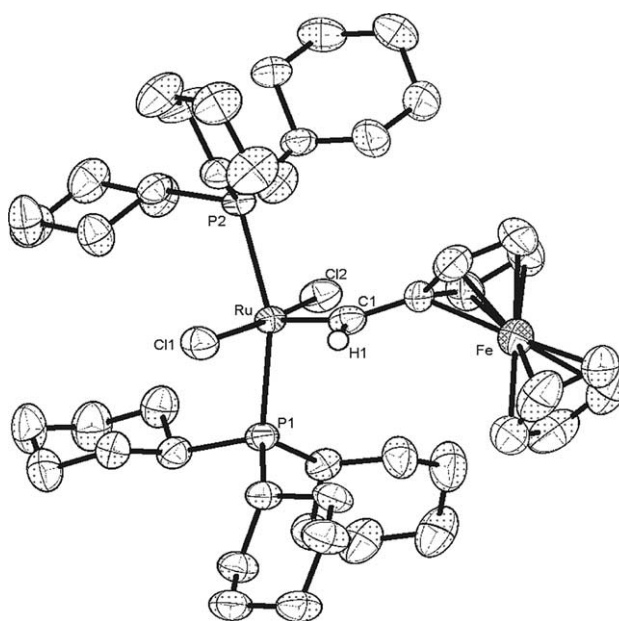
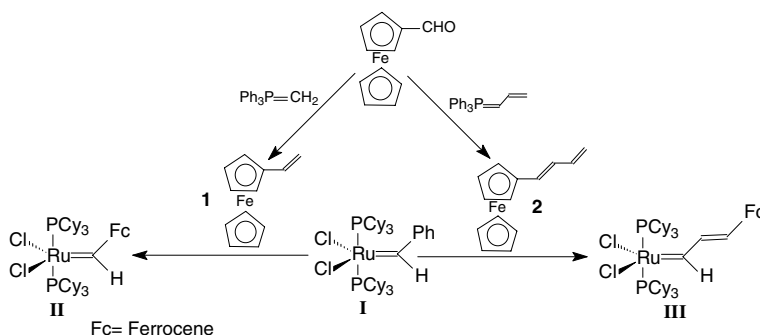
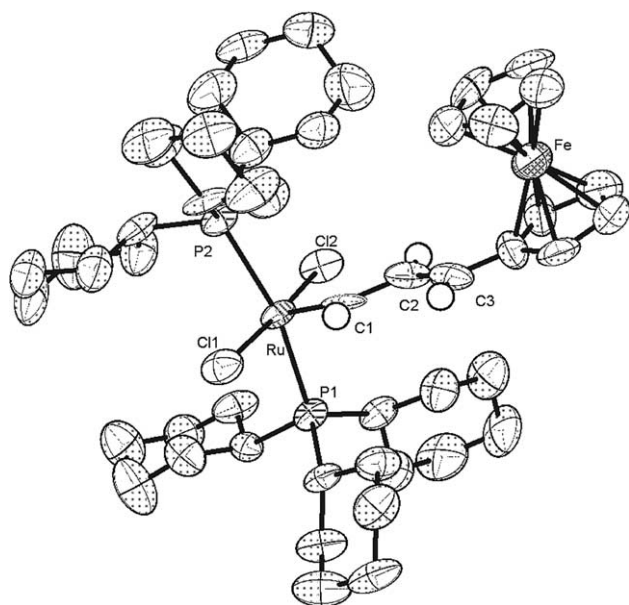


Fig. 1. ORTEP diagram of $(\text{PCy}_3)_2\text{Cl}_2\text{Ru}=\text{C}(\text{H})\text{Fc}$, **II**.



Scheme 1.

Fig. 2. ORTEP diagram of complex **III**.

parameters are summarized in Table 1. Selected bond lengths and angles are given in Table 2. The X-ray structures of **II** and **III** are similar to those of the parent complex **I**. The molecular structures reveal distorted square-pyramidal coordination with a nearly linear Cl(1)–Ru–Cl(2) angle [169.38(5)°] and [172.25(8)°] respectively for **II** and **III**. The phosphines are also found to be mutually orientated in a *trans* disposition perpendicular to the carbene moiety, as expected from NMR analyses. The Ru–C(1) bond of complex **II** [1.843(5) Å] is slightly longer than in complex **I** and average Ru–P bond is slightly longer than in complex **I**, which are believed to stem from alleviation of the increased steric and electronic congestion around the Ru center. Again, P(1)–Ru–P(2) angle of complex **II** is slightly smaller than in complex **I**, and average P–Ru–C angle of complex **II** is slightly larger, which indicate that ferrocene causes more steric crowding around the Ru center. In the case of **III**, P(1)–Ru–P(2) angle [163.91(7)°] is slightly larger and average P–Ru–C(1) angle is slightly smaller which indicate that metal center is

Table 1
Crystal data

Crystallographic data for complex II , CH ₂ Cl ₂ .		Crystallographic data for complex III	
Empirical formula	C ₄₈ H ₇₈ Cl ₄ FeP ₂ Ru	Empirical formula	C ₄₉ H ₇₈ Cl ₂ FeP ₂ Ru
Formula weight	1015.76	Formula weight	956
Temperature	293(2) K	Temperature	293(2) K
Wavelength	0.7107 Å	Wavelength	0.71073 Å
Crystal system	Triclinic,	Crystal system	Triclinic
Space group	<i>P</i> $\bar{1}$	Space group	<i>P</i> $\bar{1}$
Unit cell dimensions			
<i>a</i> (Å)	9.735(13)	<i>a</i> (Å)	12.380(2)
<i>b</i> (Å)	14.282(19)	α (°)	101.844(2)
<i>c</i> (Å)	18.704(2)	<i>b</i> (Å)	12.681(2)
α (°)	77.701(3)	β (°)	91.926(2)
β (°)	84.499(3)	<i>c</i> (Å)	16.069(2)
γ (°)	75.991(3)	γ (°)	100.109(2)
Volume	2462.5(5) Å ³	Volume	2424.3(6) Å ³
Z, Calculated density	2, 1.370 mg/m ³	Z, Calculated density	2, 1.309 mg/m ³
Absorption coefficient	0.915 mm ⁻¹	Absorption coefficient	0.818 mm ⁻¹
<i>F</i> (000)	1068	<i>F</i> (000)	1010
Crystal size (mm ³)	0.024 × 0.052 × 0.27	Crystal size (mm ³)	0.14 × 0.11 × 0.05
θ range for data collection	1.12 to 25.00°	θ range for data collection	1.30 to 25.00°
Limiting indices	–11 ≤ <i>h</i> ≤ 11, –16 ≤ <i>k</i> ≤ 16, –22 ≤ <i>l</i> ≤ 22	Limiting indices	–14 ≤ <i>h</i> ≤ 14, –15 ≤ <i>k</i> ≤ 15, –19 ≤ <i>l</i> ≤ 19
Reflections collected/unique	23,46/8620 [<i>R</i> (int) = 0.0606]	Reflections collected/unique	30,795/8522 [<i>R</i> _{int} = 0.1291]
Completeness to θ = 25.00	99.4%	Completeness to θ = 25.00	99.8%
Refinement method	Full-matrix least-squares on <i>F</i> ²	Maximum and minimum transmission	0.9587 and 0.8906
Data/restraints/parameters	8620/0/506	Refinement method	Full-matrix least-squares on <i>F</i> ²
Goodness-of-fit on <i>F</i> ²	0.991	Data/restraints/parameters	8522/0/496
Final <i>R</i> indices [<i>I</i> > 2 σ (<i>I</i>)]	<i>R</i> ₁ = 0.0566, <i>wR</i> ₂ = 0.1301	Goodness-of-fit on <i>F</i> ²	0.995
<i>R</i> indices (all data)	<i>R</i> ₁ = 0.0965, <i>wR</i> ₂ = 0.1522	Final <i>R</i> indices [<i>I</i> > 2 σ (<i>I</i>)]	<i>R</i> ₁ = 0.0744, <i>wR</i> ₂ = 0.1417
Extinction coefficient	0.0000 (4)	<i>R</i> indices (all data)	<i>R</i> ₁ = 0.1690, <i>wR</i> ₂ = 0.1730
Largest different peak and hole	0.856 and –0.662 e Å ⁻³	Largest different peak and hole	1.135 and –0.767 e Å ⁻³

Table 2
Bond lengths (Å) and angles (deg) for complex **I**, **II** and **III**

(PCy ₃) ₂ Cl ₂ Ru=C(H)Fc (II)		(PCy ₃) ₂ Cl ₂ Ru=C(H)Ph (I)		(PCy ₃) ₂ Cl ₂ Ru=C(H)C(H)C(H)Fc (III)	
<i>Bond distances (Å)</i>					
Ru–C(1)	1.843(5)	Ru–C(1)	1.839(3)	Ru–C(1)	1.804(8)
Ru–Cl(1)	2.400(1)	Ru–Cl(1)	2.401(1)	Ru–Cl(1)	2.400(2)
Ru–Cl(2)	2.394(2)	Ru–Cl(2)	2.395(1)	Ru–Cl(2)	2.386(2)
Ru–P(1)	2.407(1)	Ru–P(1)	2.397(1)	Ru–P(1)	2.403(2)
Ru–P(2)	2.433(1)	Ru–P(2)	2.435(1)	Ru–P(2)	2.411(2)
C(1)–C(2)	1.449(7)			C(1)–C(2)	1.455(10)
				C(2)–C(3)	1.331(10)
				C(3)–C(4)	1.432(11)
<i>Bond angles (°)</i>					
C(1)–Ru–Cl(1)	87.35(17)	C(1)–Ru–Cl(1)	88.7(1)	C(1)–Ru–Cl(1)	88.7(3)
C(1)–Ru–Cl(2)	103.26(17)	C(1)–Ru–Cl(2)	103.7(1)	C(1)–Ru–Cl(2)	99.0(3)
Cl(1)–Ru–Cl(2)	169.38(5)	Cl(1)–Ru–Cl(2)	167.6(1)	Cl(1)–Ru–Cl(2)	172.25(8)
C(1)–Ru–P(1)	100.86(16)	C(1)–Ru–P(1)	97.5(1)	C(1)–Ru–P(1)	97.2(2)
C(1)–Ru–P(2)	99.20(16)	C(1)–Ru–P(2)	101.2(1)	C(1)–Ru–P(2)	98.8(2)
Cl(2)–Ru–P(1)	90.89(5)	Cl(2)–Ru–P(1)	91.5(1)	Cl(2)–Ru–P(1)	87.61(7)
Cl(1)–Ru–P(1)	87.57(5)	Cl(1)–Ru–P(1)	87.2(1)	Cl(1)–Ru–P(1)	90.55(7)
Cl(2)–Ru–P(2)	88.26(5)	Cl(2)–Ru–P(2)	86.5(1)	Cl(2)–Ru–P(2)	91.32(7)
Cl(1)–Ru–P(2)	89.52(5)	Cl(1)–Ru–P(2)	90.8(1)	Cl(1)–Ru–P(2)	88.36(8)
P(1)–Ru–P(2)	159.57(5)	P(1)–Ru–P(2)	161.1(1)	P(1)–Ru–P(2)	163.91(7)

much away from ferrocene. Shorter Ru–C(1), Ru–Cl (average) and Ru–P (average) bond of **III** compare to **I** and **II** reveal that ferrocene has no steric influence on metal-center. The C(1)–C(2) bond distance [1.455(10) Å] which is shorter than a C–C single bond (1.54 Å) and C(2)–C(3) bond distance [1.331(10) Å] which, in turn is shorter than a C=C double bond (1.4 Å), imply that there is an electronic communication between the two metal center and also it indicates that ferrocene is a very good electron donor system which builds up the delocalized electron density along the butadiene linkage.

The crystal structure of **II** indicates the presence of dichloromethane as solvent of crystallization in its crystal lattice. The extended structure of complex **II** (Fig. 3) reveals two types of secondary intermolecular interactions (the cyclohexane rings attached to phosphorus are deleted for clarity in Fig. 3). In one, one of the ferrocene-H(4) has a close contact (2.799 Å) with the chlorine (Cl1) atom attached to ruthenium. In the other, one of the hydrogens (H48B) of solvent dichloromethane has a close contact (2.750 Å) with the second chlorine (Cl2) on ruthenium (Table 3). Such non-conventional hydrogen bonds may play an important role in determining the structure of metal complexes. This explains why and how dichloromethane participates in stabilizing the crystal structure as solvent of crystallization. These are examples of relatively rare M–X–HC type interaction. The observed distances lie closer to the lowest limit and the arrangement tends to be linear, indicating that these are in a relatively stronger domain of this ‘weak’ interaction. According to literature, these interactions are very importance in molecular recognition processes, the reactivity and structure of biomolecular species, the

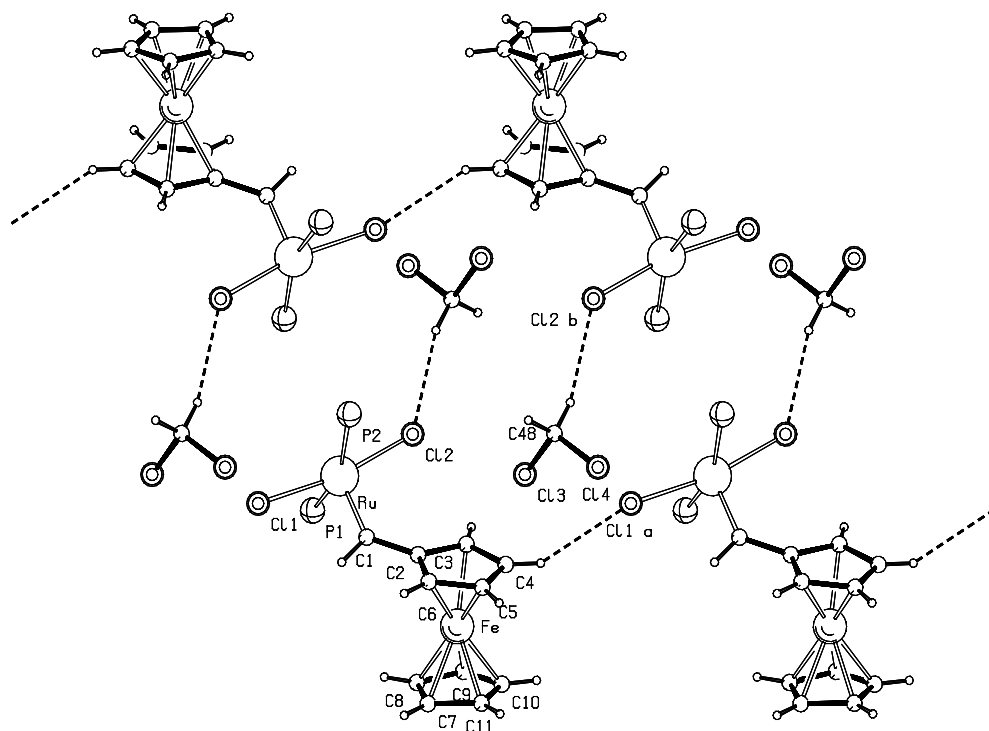
stability of inclusion complexes, crystal engineering, molecular conformation and ionic liquids [11].

2.3. Absorption spectra

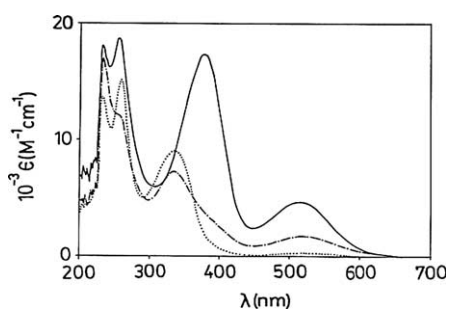
The absorption spectra of the complexes (**I–III**) in dichloromethane solvent are shown in Fig. 4 and the data are listed in Table 4. The complexes exhibit three intense transitions in the range 233–378 nm. The profile and position of the two higher energy bands (233–258 nm range) appear to be similar. The position of the lower energy band at 336 nm remains more or less same for **I** and **II**, on the other hand the same has been substantially red shifted (379 nm) in **III** with appreciable intensity enhancement due to the effect of extended conjugation in the bridging carbene unit in complex **III**. In addition, the complexes **II** and **III** display one moderately intense transition in the visible region (near 520 nm) and the intensity substantially increases with the increase in conjugation in the carbene framework on moving from **II** to **III**. However, complex **I** displays a very weak transition at 520 nm. Therefore, the origin of the lowest energy transition is not clear at present.

2.4. Electrochemistry

The redox properties of the complexes (**I**, **II** and **III**) have been studied in dichloromethane by cyclic voltammetric and differential pulse voltammetric techniques using platinum wire working electrode. The voltammograms are shown in Fig. 5 and the potentials are set in Table 5. Potentials are recorded against saturated calomel electrode (SCE) as reference.

Fig. 3. Extended structure of complex **II**. CH₂Cl₂.Table 3
Data for two secondary Intermolecular interactions

Donor-H...Acceptor	D-H (Å)	H...A (Å)	D...A (Å)	D-H...A (°)
C(4)-H(4)...Cl(1) ⁱ	0.9300	2.7994	3.6333	149.79
C(48)-H(48B)...Cl(2) ⁱⁱ	0.9700	2.7500	3.6866	162.47

Equivalent Position Code $i = 1 + x, y, z$; $ii = 1 - x, 1 - y, 1 - z$.Fig. 4. Absorption spectra of complexes **I** (···), complex **II** (---), complex **III** (—) in dichloromethane solvent.Table 4
Absorption spectral data in dichloromethane solvent at 298 K

Compound	λ/nm ($\epsilon/\text{M}^{-1}\text{cm}^{-1}$)
I	520 (360), 336 (9060), 255 (15500), 236 (13700)
II	516 (1915), 334 (8044), 258 (13382), 234 (17443)
III	518 (4630), 379 (17479), 256 (18800), 233 (17978)

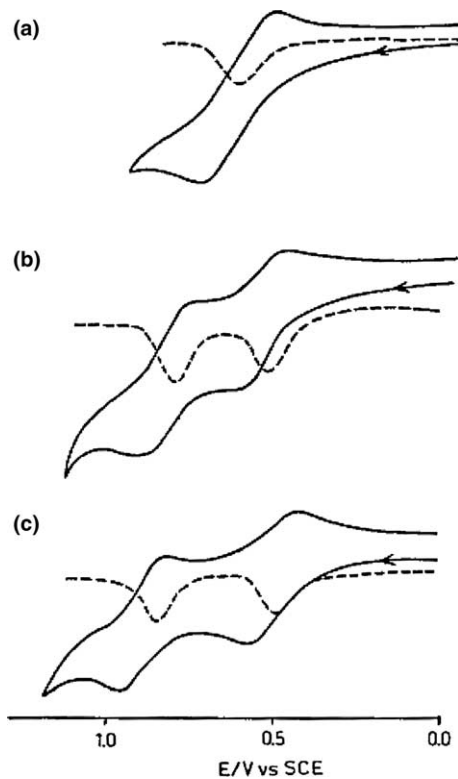
Fig. 5. Cyclic voltammograms (---) and differential pulse voltammograms (—) of (a) complex **I**; (b) complex **II** and (c) complex **III** in dichloromethane solvent.

Table 5
Electrochemical data at 298 K^a

Complex	E_{298}^0 , V (ΔE_p , mV)	
	Fe ^{III} -Fe ^{II}	Ru ^{III} -Ru ^{II}
I	–	0.70(130)
II	0.55(110)	0.84(100)
III	0.51(130)	0.88(140)

^a Condition: solvent, dichloromethane; supporting electrolyte, TEAP; reference electrode, SCE; solute concentration, $\sim 10^{-3}$ M; scan rate 50 mv/s; working electrode, platinum wire.

Mononuclear Ru(II) complex **I** exhibits one quasi-reversible Ru(III)–Ru(II) couple at 0.70 V vs. SCE (Fig. 5(a)) [12]. However, complex **II**, where the same Ru^{II}(PCy₃)₂Cl₂ unit is linked with a ferrocenylidene moiety, shows two successive one-electron oxidation processes at 0.55 and 0.84 V vs. SCE. The first one is assigned to oxidation of Fe(II) center of ferrocene to Fe(III) [13a] (Under identical experimental conditions the ferrocene/ferrocenium couple appears at 0.49 V vs. SCE). The higher potential of 0.84 V pertains to oxidation of Ru(II) center, oxidation of which has been rendered more difficult (the Ru(III)–Ru(II) potential increases by 140 mV) by oxidation of Fe(II) center prior to oxidation at ruthenium [13a,b,d] (Fig. 5b).

The complex **III** incorporating a 1,3-butadiene bridge between ruthenium and iron, exhibits two successive one-electron oxidation processes corresponding to Fe(II)–

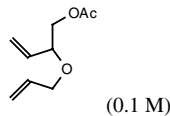
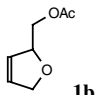
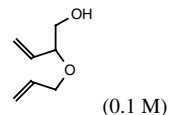
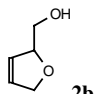
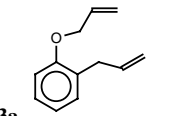
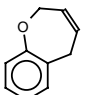
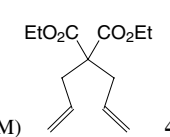
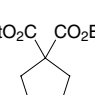
Fe(III) and Ru(II)–Ru(III) couples at 0.51 and 0.88 V respectively (Fig. 5(c)). In this case the separation in potential between the couples is 370 mV, significantly greater than the difference observed for complex **II** (290 mV). This is consistent with electronic communication between the metal centers through the π -framework extending from Cp ring of ferrocene to the C=Ru bond [13a,c].

The existence of conjugated butadiene bridge between the metal centers in **III** provides higher degree of intermetallic coupling which is essentially reflected in the observed larger separation in potentials for the successive metal-based redox processes in **III** [14].

2.5. RCM-activity of complex **II** and **III**

The close similarity of structure of complex **II** with Grubbs' metathesis catalyst **I** prompted an assessment of the former as possible catalyst for alkene metathesis. It was recognized that after the first cycle, there would be no difference between the catalytically significant intermediates generated from either **I** or **II** or **III**. Only the initiation rates might differ due to variation in carbene substituent [8]. In the present case, the steric bulk of ferrocene and its ability to act as an electron-donor, would favor dissociation of a tricyclohexylphosphine and complexation of smaller alkene molecule over bulky phosphine at the vacant coordination site.

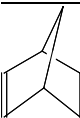
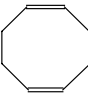
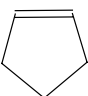
Table 6
RCM using catalyst **II** and **III**^a

Entry	Substrates (Conc.)	Product	Catalyst (mol%)	Time/Temp	Yield (%) ^b
1	 1a (0.1 M)	 1b	2.5	15 min/room temperature	98 (97)
2	 2a (0.1 M)	 2b	2.5	2 h/room temperature	90 (93)
3	 3a (0.05 M)	 3b	2.5	30 min/room temperature	98 (97)
4	 4a (0.1 M)	 4b	5	2 h/reflux	94 (96)

^a All the reactions were carried out in 1-2 mmol scale in CH₂Cl₂ under Ar.

^b Numbers within the parenthesis are the yields of RCM reactions using complex **III** as a catalyst.

Table 7
ROMP of various cyclic olefins^a

Monomer	M/C ^b	<i>t</i> (h)	Yield (%)	<i>M_n</i>	<i>M_w</i>	PDI ^c
	10000	1.5	85	148,620	239,450	1.6
	1000	1.5	98	119,120	207,180	1.7
	1000	24	95	18,200	27,540	3.2
	10000	2.5	— ^d	— ^d	— ^d	— ^d
	1000	2.5	57	94,770	159,100	1.7
	1000	24	79	67,635	141,510	2.0
	10000	1.5	48	56,165	83,220	1.4
	1000	1.5	58	7,160	12,800	1.8
	1000	24	65	54,360	117,000	2.1

^a Bulk polymerizations using catalyst **II** at room temperature; (monomer)₀ = 4.5 M in dichloromethane.

^b Initial monomer/catalyst molar ratio.

^c Determined by GPC (CHCl₃) and results are reported relative to poly(styrene) standards.

^d No polymer was obtained as a solid precipitate, the experiment was repeated thrice with same result.

Indeed, the complexes **II** [8c] and **III** displayed significant and comparable catalytic activity in ring-closing metathesis (RCM) reaction as seen from representative results summarized in Table 6. The yields are generally excellent while the reaction time is short. Efficiency of these catalysts is comparable with Grubbs' first-generation catalyst **I** (Yield: 98% for **1a** and 95–99% for **4a** under similar condition) [15]. The propagation steps are identical for all the catalysts (**I–III**), which differ only in the initiation step. Substrates with free hydroxyl groups seem to require a longer period for complete conversion than corresponding acetates.

2.6. ROMP activity of complex **II**

Success with RCM prompted a study of ring-opening metathesis polymerization (ROMP) with these new complexes. Initial results with representative cycloalkenes initiated by complex **II** were encouraging.

Complex **II** was found to be an active ROMP catalyst [16] for both moderately and highly strained cycloalkene monomers (Table 7). Typically, polymerization was performed in dichloromethane (3–4.5 M) at ambient temperature. The reaction mixture became viscous within few minutes and the color of the catalyst changed from reddish to pink. After few hours, the reaction mixture was exposed to air and treated with excess dichloromethane and ethyl vinyl ether (containing traces of an antioxidant, 2, 6-di-*tert*-butyl-4-methylphenol) as a quenching agent. The resulting solution was stirred for a few minutes. After filtration through a short column of silica gel, it was poured into a beaker containing vigorously stirred methanol when the product was precipitated as white solid.

The strained monomer like norbornene yielded high yield of polymer compared to cycloocta-1,5-diene and cyclopentene that are less strained. The amount of

norbornene in excess of the ratio 1000/1 does not seem to have a significant impact. Also, the PDI increased if the reaction was allowed to continue for long period (24 h). Together these data imply that chain transfer is a slower process than propagation. It is unclear, however, why a ratio of 10,000/1 of cycloocta-1,5-diene/catalyst failed to yield polymers of high molecular weight.

3. Conclusion

In summary, we have described synthesis of new, bimetallic derivatives **II** and **III** made up of a ferrocene and a ruthenium carbene fragment by a simple and facile route using alkene metathesis as the key transformation. These are prototypical of a wide range of complexes that can be synthesized in a similar way. Crystal structures of **II** and **III** have been solved. Crystal structure of **II** revealed a network of [Ru]Cl–H–C type of weak bonds, a relatively rare occurrence, that involve dichloromethane (solvent of crystallization) and ferrocene as partners. Electrochemical studies indicate there is a clear communication between the metal centers through the molecular π -framework. Interestingly, the complex **II** is catalytically active for both RCM and ROMP, and promises to provide ferrocene-tethered polymer chains as interesting materials if a 'living' system can be developed.

4. Experimental section

4.1. General procedures and methods

All manipulations were carried out under argon atmosphere. The solvents were dried according to

established procedure; complex **I** was prepared following the reported [9] procedure; ferrocene and all other chemicals were used as purchased from Aldrich or Lancaster. NMR spectra were recorded on a Bruker AC200, MSL300 or DRX500 spectrometer. The ^1H NMR, ^{13}C NMR and ^{31}P nuclei were studied at 200 or 500, 50.32 and 125.76, 81.02 and 202.46 MHz respectively. IR spectra were recorded on a Perkin–Elmer Paragon 1000 FT-IR spectrometer. Elemental analyses were performed on a Carlo-Erba 1100 automatic analyzer at NCL micro-analysis facility. Absorption spectra of the complexes were recorded using Shimadzu 2100 UV–Visible spectrophotometer at 298 K in dichloromethane solvent. Electrochemical measurements were carried out using a PAR model 273A potentiostat/galvanostat. A platinum wire working electrode (length 0.3 cm and diameter 0.5 mm), a platinum wire auxiliary electrode and a saturated calomel reference electrode (SCE) were used in a three-electrode configuration. The half wave potential E_{298}^0 was set equal to 0.5 ($E_{\text{pa}} + E_{\text{pc}}$), where E_{pa} and E_{pc} are anodic and cathodic cyclic voltammetric peak potentials, respectively. Molecular weight and molecular weight distribution (MWD) of the oligomers were determined using a Thermofinnigan gel permeation chromatograph equipped with a refractive index detector and μ -styragel columns (10^5 to 50 Å), based on polystyrene standards at 25 °C using chloroform as the solvent with one mL/min flow rate. The data was processed using the software PSS WinGPC Scientific.

4.2. Preparation of 1-ferrocenyl-1,3-butadiene (**2**)

A solution of ferrocenecarboxaldehyde (200 mg, 0.93 mmol) in dry THF (5 mL) was stirred at -78 °C. A freshly prepared solution of ylide [prepared from allyl-triphenylphosphonium bromide (800 mg, 2 mmol) and *n*-BuLi (1 mL of 1.54 M, 1.5 mmol) in THF (15 mL) was added. Stirring was continued at room temperature for 3 h. THF was evaporated and ethyl acetate (25 mL) was added followed by quenching with water (10 mL). Organic layer was washed with brine solution. The solvent was removed under reduced pressure and the residue was purified by flash chromatography. The product was a semi-solid, reddish yellow compound. Yield = 198 mg (89%).

4.3. Preparation of $(\text{PCy}_3)_2\text{Cl}_2\text{Ru}=\text{C}(\text{H})\text{Fc}$ (**II**)

Vinylferrocene **1** (61 mg, 0.29 mmol) in 1 mL dichloromethane was added to a solution of Ru-benzylidene complex **I** (200 mg, 0.243 mmol) in dichloromethane (5 mL). The reaction mixture was stirred at room temperature for 40 min when the solution turned purple to red–violet. Volume of the solvent was reduced followed by addition of dry methanol at 0 °C, which affor-

ded $(\text{PCy}_3)_2\text{Cl}_2\text{Ru}=\text{C}(\text{H})\text{Fc}$ **II** as dark brown solid powder in 87% yield (198 mg). ^1H NMR (CD_2Cl_2): δ 19.00 (s, 1H, Ru=CH), 4.70 (s, 2H, Cp), 4.43 (s, 2H, Cp), 4.14 (s, 5H, Cp), 2.54 (broad s, 6H, PCy_3), 1.21–1.74 (m, 60H, PCy_3). ^{13}C NMR (CD_2Cl_2): δ 292.1, 104.2, 71.5, 71.2, 69.8, 32.7, 32.0, 30.1, 28.4, 27.0. ^{31}P NMR (CD_2Cl_2): δ 34.4 (s, PCy_3). IR (CHCl_3 , cm^{-1}): 2931, 2852, 1444, 1265, 1004. M.p.: 135 °C (dec.). Anal. Calc. for $\text{C}_{47}\text{H}_{76}\text{Cl}_2\text{FeRuP}_2 \cdot \text{CH}_2\text{Cl}_2$: C, 56.74; H, 7.68. Found: C, 57.6; H, 7.68%.

4.4. Preparation of $(\text{PCy}_3)_2\text{Cl}_2\text{Ru}=\text{C}(\text{H})\text{C}(\text{H})=\text{C}(\text{H})\text{Fc}$ (**III**)

1-ferrocenylbuta-1,3-diene **2** (60 mg, 0.252 mmol) in 1 mL dichloromethane was added to a solution of Ru benzylidene complex **I** (200 mg, 0.243 mmol) in dichloromethane (5 mL). The reaction was stirred at room temperature for 40 min during which the solution turned purple to red–violet. Volume of the solvent was reduced followed by addition of dry methanol at 0 °C, which afforded $(\text{PCy}_3)_2\text{Cl}_2\text{Ru}=\text{C}(\text{H})\text{C}(\text{H})=\text{C}(\text{H})\text{Fc}$ **III** as dark brown solid powder in 92% yield (215 mg). ^1H NMR (CDCl_3): δ 18.55–18.50 (d, 1H, $J = 10$ Hz, Ru=CH), 8.07–8.20 (m, 1H), 7.28–7.33 (d, 1H, $J = 10$ Hz), 4.60 (s, 2H, Cp), 4.48 (s, 2H, Cp), 4.16 (s, 5H, Cp), 2.64 (broad m, 6H, Cy), 1.26–1.86 (m, 60H, Cy). ^{13}C NMR (CDCl_3): δ 288.9, 144.5, 135.2, 81.2, 71.3, 69.4, 68.6, 32.1, 29.6, 27.8, 26.5. ^{31}P NMR (CDCl_3): δ 35.13 (s, PCy_3). IR (CHCl_3 , cm^{-1}): 2931, 2852, 1569, 1446, 1107, 1004. mp 137 °C (dec.). Anal. Calc. for $\text{C}_{47}\text{H}_{76}\text{Cl}_2\text{FeRuP}_2$: C, 61.5; H, 8.15. Found: C, 60.93; H, 8.14%.

4.5. X-ray crystal structure analysis for complex **II**

4.5.1. Crystal data

Single crystals of the complex were grown by slow diffusion of methanol into the concentrated solution of complex **II** in dichloromethane at low temperature (-78 °C). Dark brown coloured tiny crystal of approximate size $0.024 \times 0.052 \times 0.270$ mm, was used for data collection on Bruker SMART APEX CCD diffractometer using Mo $\text{K}\alpha$ radiation, fine focus tube with 50 kV and 40 mA. Crystal to detector distance 6.05 cm, 512×512 pixels/frame, Quadrant data acquisition. Total scans = 4, total frames = 2424, Oscillation/frame -0.3° , exposure/frame = 30.0 s/frame, maximum detector swing angle = -30.0° , beam center = (260.2, 252.5), in plane spot width = 1.24, SAINT integration, θ range = 1.11 to 25° , completeness to θ of 25° is 99.4%. SADABS correction applied, $\text{C}_{47}\text{H}_{76}\text{Cl}_2\text{FeP}_2\text{Ru} \cdot \text{CH}_2\text{Cl}_2$, FW = 1015. Crystals belong to triclinic, space group $\bar{P}1$, $a = 9.735(1)$ Å, $b = 14.282(2)$ Å, $c = 18.704(2)$ Å, $\alpha = 77.701(3)^\circ$, $\beta = 84.499(3)^\circ$, $\gamma = 75.991(3)^\circ$, $V = 2462.5(5)$ Å³, $Z = 2$, $D_c = 1.37$

mg/m⁻³, μ (Mo–K) = 0.915 mm⁻¹, T = 293(2) K, 23746 reflections measured, 8620 unique [$I > 2\sigma(I)$], R value 0.0566, wR_2 = 0.1301. All the data were corrected for Lorentzian, polarisation and absorption effects. SHELX-97 (ShelxTL) [17] was used for structure solution and full matrix least squares refinement on F^2 . Hydrogen atoms were included in the refinement as per the riding model. Data collection and refinement parameters are listed in Table 1. ORTEP diagram of the molecule is included in Fig. 1. Ellipsoids are drawn at 40% probability. The complex **II** contains a DCM molecule as a solvent of crystallization. Crystallographic data for the structural analysis has been deposited with the Cambridge Crystallographic Data Centre, CCDC No. 203959 for the complex **II**.

4.6. X-ray crystal structure analysis for complex **III**

4.6.1. Crystal data

Single crystals of the complex were grown by slow removal of dichloromethane from the methanol–dichloromethane (3:1) solution of **III**. Dark brown thin needles of approximate size 0.14 × 0.11 × 0.05 mm, was used for data collection on Bruker SMART APEX CCD diffractometer using Mo K α radiation, fine focus tube with 50 kV and 30 mA. Crystal to detector distance 6.05 cm, 512 × 512 pixels/frame, Multirun data acquisition. Total scans = 6, total frames = 3636, Oscillation/frame –0.3°, exposure/frame = 30.0 s/frame, maximum detector swing angle = –30.0°, beam center = (260.2, 252.5), in plane spot width = 1.24, SAINT integration, θ range = 1.30–25°, completeness to θ of 25° is 99.8%. SADABS correction applied, C₄₉H₇₈Cl₂FeP₂Ru, FM = 956. Crystals belong to triclinic, space group $P\bar{1}$, a = 12.380(2), b = 12.681(2), c = 16.069(2) Å, α = 101.844(2), β = 91.926(2), γ = 100.109(2)°, V = 2424.3(6) Å³, Z = 2, D_c = 1.309 mg/m³, μ (Mo–K) = 0.818 mm⁻¹, T = 293(2) K, 30795 reflections measured, 8522 unique [$I > 2\sigma(I)$], R value 0.0744, wR_2 = 0.1417. All the data were corrected for Lorentzian, polarization and absorption effects. SHELX-97 (ShelxTL) [17] was used for structure solution and full matrix least squares refinement on F^2 . Hydrogen atoms were included in the refinement as per the riding model. Data collection and refinement parameters are listed in Table 1. ORTEP diagram of the molecule is included in Fig. 2. Ellipsoids are drawn at 40% probability. Crystallographic data for the structural analysis has been deposited with the Cambridge Crystallographic Data Centre, CCDC No. 249344 for the complex **III**.

4.7. RCM with complex **II** and **III** as catalysts

Complex **II** or **III** (0.025 mmol, 2.5%) in anhydrous dichloromethane (3 mL) was added to a solution of

1.0 mmol of **1a–4a** in anhydrous dichloromethane (7 mL) under argon. The reaction mixture (0.1 M) was stirred at room temperature (or heated under reflux) and monitored by TLC. After the reaction was complete, solvent was removed under reduced pressure and the residue was chromatographed (Acetone/Pet-ether 1:20) to afford the pure product, **1b–4b**. Formation of product was indicated by the disappearance of signals due to the terminal olefinic group (=CH₂) in the NMR spectra.

1b: Colorless liquid. ¹H NMR (CDCl₃): δ 5.99–6.02 (1H, m), 5.72–5.75 (1H, m), 4.95–5.03 (1H, m), 4.64–4.70 (2H, m), 4.01–4.20 (2H, m), 2.07 (3H, s). ¹³C NMR (CDCl₃): δ 171.1, 129.2, 125.9, 84.3, 75.7, 66.4, 20.9. IR (CHCl₃, cm⁻¹): ν 2954, 2858, 1743, 1436, 1375, 1236, 1087, 1041. Mass (m/z): 126 (M).

2b: Colorless liquid. ¹H NMR (CDCl₃): 5.99–6.03 (1H, m), 5.74–5.77 (1H, m), 4.91 (1H, bs), 4.67–4.73 (2H, m), 3.52–3.76 (2H, m), 2.29 (1H, s). ¹³C NMR (CDCl₃): δ 128.6, 126.4, 86.9, 75.5, 65.0. IR (CHCl₃, cm⁻¹): ν 3417, 2921, 2858, 1652, 1450, 1417, 1355, 1074, 1037. Mass (m/z): 100 (M).

3b: Colorless liquid. ¹H NMR (CDCl₃): δ 7.07–7.25 (4H, m), 5.90–5.93 (1H, m), 5.52–5.54 (1H, m), 4.65 (2H, s), 3.55 (2H, s). ¹³C NMR (CDCl₃): δ 158.7, 136.0, 128.7, 127.8, 127.3, 125.8, 123.9, 121.4, 71.1, 31.8. IR (CHCl₃, cm⁻¹): ν 3022, 2931, 2842, 1583, 1490, 1230, 1062. Mass (m/z): 146 (M).

4.8. ROMP with complex **II** as catalyst

In a typical procedure, norbornene (490 mg, 5.2 mmol) was taken in dichloromethane (9 mL) and treated with **II** (4.8 mg, 5.2 × 10⁻³ mmol) in dichloromethane (3 mL) at room temperature. The reaction mixtures became viscous within 3–5 min and the color changed from brown–green to orange. The solutions were stirred at room temperature for 1.5 h, then exposed to air and treated with dichloromethane (10 mL) containing traces of 2,6-di-*tert*-butyl-4-methylphenol and ethyl vinyl ether. The resulting green solution was stirred for 25 min and, after filtration through short columns of silica gel, poured into vigorously stirred methanol (200 mL). White, tacky polymers were obtained which were isolated, washed twice with methanol, and dried under vacuum. Yield = 482 mg (98%, ~90% *trans*), PDI (CHCl₃) = 1.7.

Acknowledgements

The author (TKM) wishes to thank CSIR, Govt. of India, for research fellowships and Reliance Industries Ltd. for financial assistance.

Appendix A. Supplementary data

Supplementary data associated with this article can be found, in the online version at [doi:10.1016/j.jorganchem.2004.11.012](https://doi.org/10.1016/j.jorganchem.2004.11.012).

References

- [1] (a) C.P. Casey, R.M. Bullock, W.C. Fultz, A.L. Rheingold, *Organometallics* 1 (1982) 1591;
 (b) G.J. Baird, S.G. Davis, S.D. Moon, S.J. Simpson, R.H. Jones, *J. Chem. Soc., Dalton Trans.* (1985) 1479;
 (c) C.L. Sterzo, J.K. Stille, *Organometallics* 9 (1990) 687;
 (d) C.L. Sterzo, *Organometallics* 9 (1990) 3185;
 (e) R.M. Bullock, F.R. Lemke, D.J. Szalda, *J. Am. Chem. Soc.* 112 (1990) 3244;
 (f) K.G. Frank, J.P. Selegue, *J. Am. Chem. Soc.* 112 (1990) 6414;
 (g) F.R. Lemke, D.J. Szalda, R.M. Bullock, *J. Am. Chem. Soc.* 113 (1991) 8466;
 (h) P.H. van Rooyen, M. Schindehutte, S. Lotz, *Organometallics* 11 (1992) 1104;
 (i) M.J. Doyle, T.J. Duckworth, L. Manojlovic-Muir, M.J. Mays, P.R. Raithby, F.J. Robertson, *J. Chem. Soc., Dalton Trans.* (1992) 2703;
 (j) S. Lotz, M. Schindehutte, P.H. van Rooyen, *Organometallics* 11 (1992) 629;
 (k) M. Herberhold, W. Feger, U. K611e, *J. Organomet. Chem.* 436 (1992) 333.
- [2] (a) A.F. Diaz, U.T. Mueller-Westerhoff, A. Nazzal, M. Tanner, *J. Organomet. Chem.* 236 (1982) C45;
 (b) S.B. Colbran, B.H. Robinson, J. Simpson, *Organometallics* 2 (1983) 943–952;
 (c) J. Kotz, G. Neyhart, W.J. Vining, M.D. Rausch, *Organometallics* 2 (1983) 79;
 (d) J.C. Kotz, E.E. Getty, L. Lin, *Organometallics* 4 (1985) 610;
 (e) D.A. Clemente, G. Pilloni, B. Corain, B. Longato, M. Tiripicchio-Camellini, *Inorg. Chim. Acta* 115 (1986) L9;
 (f) D. Obendorf, H. Schottenberger, C. Rieker, *Organometallics* 10 (1991) 1293;
 (g) Y. Kasahara, Y. Hoshino, M. Kajitani, K. Shimizu, G.P. Sato, *Organometallics* 11 (1992) 589.
- [3] (a) D.B. Brown (Ed.), *Mixed-Valence Compounds*, D. Reidel Publishing Co, Dordrecht, Holland, 1980;
 (b) C.U. Pittmann Jr., B. Suryanarayanan, *J. Am. Chem. Soc.* 96 (1974) 7916.
- [4] (a) T.J. Meyer, *Acc. Chem. Res.* 22 (1989) 163;
 (b) J.S. Connolly, *Photochemical Conversion and Storage of Solar Energy*, Academic Press, New York, 1981.
- [5] (a) For reviews, see N.J. Long, *Angew. Chem. Int. Ed. Engl.* 34 (1995) 21;
 (b) S. Barlow, S.R. Marder, *J. Chem. Soc., Chem. Commun.* (2000) 1555;
 (c) , For an example reported from this laboratory, see K.N. Jayaprakash, P.C. Ray, I. Matsuoka, M.M. Bhadbhade, V.G. Puranik, P.K. Das, H. Nishihara, A. Sarkar, *Organometallics* 18 (1999) 3851.
- [6] (a) P.D. Beer, O. Kocian, *J. Chem. Soc., Dalton Trans.* (1990) 3283;
 (b) I.R. Butler, *Organometallics* 11 (1992) 74;
 (c) M. Sato, Y. Hayashi, S. Kumakura, N. Shimizu, M. Katada, S. Kawata, *Organometallics* 15 (1996) 721;
 (d) N. Dowling, P.M. Henry, N.A. Lewis, H. Taube, *Inorg. Chem.* 20 (1981) 2345;
 (e) N. Dowling, P.M. Henry, *Inorg. Chem.* 21 (1982) 4088.
- [7] (a) J.C. Calabrese, L.-T. Cheng, J.C. Green, S.R. Marder, W. Tam, *J. Am. Chem. Soc.* 113 (1991) 7227;
 (b) H.E. Bunting, M.L.H. Green, S.R. Marder, M.E. Thompson, D. Bloor, P.V. Kolinsky, R.J. Jones, *Polyhedron* 11 (1992) 1489;
 (c) S. Ghosal, M. Samoc, P.N. Prasad, J.J. Tufariello, *J. Phys. Chem.* 94 (1990) 2847.
- [8] (a) For a collection of Ru-based initiators, see U. Frenzel, O. Nuyken, *J. Polym. Sci. A* 40 (2002) 2895;
 (b) , For a very recent report, see J. Louie, R.H. Grubbs, *Organometallics* 21 (2002) 2153;
 (c) , Preliminary report on catalytic activity of complex II for RCM, etc. T.K. Maishal, A. Sarkar, *SynLett.* 11 (2002) 1925.
- [9] P. Schwab, R.H. Grubbs, J.W. Ziller, *J. Am. Chem. Soc.* 118 (1996) 100.
- [10] (a) S.-J. Jong, J.-M. Fang, *J. Org. Chem.* 66 (2001) 3533;
 (b) J.M. Osgerby, P.L. Pauson, *J. Chem. Soc.* (1961) 4604;
 (c) B.W. Ponder, R.C. Kneisel, D.H. Lewis, *Org. Prep. Proc. Int.* 3 (1971) 171;
 (d) D.H. Lewis, M.C. Neal, B.W. Ponder, *Synth. Commun.* 2 (1972) 93.
- [11] (a) C.B. Aakeröy, T.A. Evans, K.R. Seddon, I. Pálinkó, *New J. Chem.* (1999) 145;
 (b) M. Freytag, P.G. Jones, *J. Chem. Soc., Chem. Commun.* (2000) 277;
 (c) G. Aullon, D. Bellamy, L. Brammer, E.A. Bruton, A.G. Orpen, *J. Chem. Soc., Chem. Commun.* (1998) 653.
- [12] G.K. Lahiri, S. Bhattacharya, M. Mukherjee, A.K. Mukherjee, A. Chakravorty, *Inorg. Chem.* 26 (1987) 3359.
- [13] (a) For electrochemistry of mixed valence complexes featuring ferrocene and Ru(II), see M. Sato, H. Shintate, Y. Kawata, M. Sekino, *Organometallics* 13 (1994) 1956;
 (b) N.D. Jones, M.O. Wolf, *Organometallics* 16 (1997) 1352;
 (c) P. Štěpnička, R. Gyepes, *Organometallics* 16 (1997) 5089;
 (d) K.R.J. Thomas, J.T. Lin, H.-M. Lin, C.-P. Chang, C.-H. Chuen, *Organometallics* 20 (2001) 557.
- [14] B. Sarkar, R.H. Laye, B. Mondal, S. Chakraborty, R.L. Paul, J.C. Jeffery, V.G. Puranik, M.D. Ward, G.K. Lahiri, *J. Chem. Soc., Dalton Trans.* (2002) 2097.
- [15] (a) T.K. Maishal, D.K. Sinha-Mahapatra, K. Paranjape, A. Sarkar, *Tetrahedron Lett.* 43 (2002) 2263;
 (b) Y.M. Ahn, K.L. Yang, G.I. Georg, *Org. Lett.* 3 (2001) 1411.
- [16] (a) Selected precedents of ROMP by ruthenium carbene complexes C.W. Bielawski, R.H. Grubbs, *Angew. Chem. Int. Ed.* 39 (2000) 2902;
 (b) B.R. Maughon, R.H. Grubbs, *Macromolecules* 30 (1997) 3459;
 (c) D.-J. Liaw, J.-S. Tsai, P.-L. Wu, *Macromolecules* 33 (2000) 6925;
 (d) J. Gratt, R.E. Cohen, *Macromolecules* 30 (1997) 3137;
 (e) M.A. Hillmyer, S.T. Nguyen, R.H. Grubbs, *Macromolecules* 30 (1997) 3459;
 (f) D.A. Robson, V.C. Gibson, R.G. Davies, M. North, *Macromolecules* 32 (1999) 6371.
- [17] G.M. Sheldrick, SHELX-7 program for crystal structure solution and refinement, University of Göttingen, Germany, 1997.